AUT Journal of Modeling and Simulation

AUT J. Model. Simul., 58(1) (2026) 67-94
DOI: 10.22060/miscj.2026.24244.5413

Innovative Vehicle Routing Strategies for Pharmaceutical Distribution Using Parcel Lockers: A Bi-objective Two-Stage Stochastic Approach

Reyhaneh Shafiee Aghdam, Mohsen Akbarpour Shirazi*, Behrooz Karimi

Department of Industrial Engineering and Management Systems, Amirkabir University of Technology, Tehran, Iran.

ABSTRACT: Last-mile pharmaceutical distribution must reconcile logistics cost, delivery responsiveness, and cold-chain safety under uncertain demand. This study develops a bi-objective two-stage stochastic vehicle-routing model that integrates direct home delivery with consolidated delivery through smart parcel lockers. Vehicle reservation and locker activation are decided before demand is observed, whereas vehicle dispatch, routing, channel assignment, service timing, and multi-product flows adapt to each scenario. The model distinguishes cold-chain from ordinary products, enforces direct delivery for temperature-sensitive items, and captures a heterogeneous fleet, simultaneous delivery and pickup, locker capacity, coverage limits, and time-window-based customer satisfaction. The augmented ε-constraint (AEC) method generates exact efficient solutions for tractable instances, while a scenario-aware NSGA-II solves larger cases. Across five common benchmarks, NSGA-II is approximately 4.1 times faster; across 15 paired instances, it produces 34.5% more non-dominated solutions on average, while AEC retains a significantly lower mean ideal distance. A real pharmaceutical-distribution case in Tehran with 250 customers shows that an all-direct policy increases total cost by 11% and decreases customer satisfaction by 13.17% relative to the mixed strategy. The results also support a locker coverage radius no greater than 3 km and demonstrate substantial resilience to locker- and distance-cost changes in operationally realistic urban logistics settings.

Review History:

Received: Jun. 09, 2025
Revised: Jul. 18, 2026
Accepted: Jul. 19, 2026
Available Online: Jul. 20, 2026

Keywords:

Vehicle Routing
Last-Mile Delivery
Parcel Locker
Pharmaceutical Industry
Stochastic Programming
Bi-Objective Optimization
AEC & NSGA-II

1- Introduction

Global supply chains have faced sharp disruptions while online retail has continued to expand, making lower logistics costs and reliable delivery central operational priorities (Risberg, 2022). Last-mile delivery is commonly the most expensive and least efficient stage of the supply chain, and its performance is especially consequential for pharmaceuticals, where delays can compromise access and service quality (Kadadha et al., 2024). Demand volatility further complicates planning because a route and capacity plan based on a single forecast may become infeasible or unnecessarily expensive when realized demand changes (Qian et al., 2022).

Traditional door-to-door delivery is increasingly strained by urban congestion, high transport cost, long routes, and repeated customer stops (Pronello et al., 2017). Smart parcel lockers provide an out-of-home alternative in which multiple parcels are consolidated at an accessible location. Consolidation can reduce vehicle travel and failed-delivery risk while offering customers flexible collection times (Pinchasik et al., 2023). In pharmaceutical services, contactless medication lockers also proved valuable during the COVID-19 pandemic by reducing waiting and direct contact while maintaining access to medicines (Yeo et al., 2021).

The pharmaceutical setting nevertheless prevents a direct transfer of conventional e-commerce locker models. Temperature-sensitive products cannot be placed in non-refrigerated lockers; customers may require simultaneous delivery and collection of returns; heterogeneous vehicles and multiple product classes must share limited capacity; and service quality depends not only on time, but also on walking distance and shipping charge. These interactions create a decision problem in which the delivery channel, route, capacity allocation, and service schedule must be optimized jointly under uncertainty.

Existing studies have examined parcel-locker location, home-or-locker routing, healthcare pickup systems, and stochastic routing separately. However, the comparison in Table 1 shows that prior work has not jointly integrated pharmaceutical cold-chain restrictions, direct-versus-locker assignment at the customer-product level, heterogeneous multi-product vehicle routing with returns, two-stage demand recourse, and an explicit cost–satisfaction trade-off. The contribution is therefore not the use of a standard vehicle-routing or evolutionary method alone; it is the integrated stochastic decision architecture and its validation in a

*Corresponding author’s email: akbarpour@aut.ac.ir

pharmaceutical distribution network.

The study makes the following contributions:

- Developing an integrated pharmaceutical routing model that assigns each customer-product to direct or locker delivery while enforcing direct service for cold-chain items and preserving locker consolidation.
- Introducing a two-stage stochastic architecture in which only vehicle reservation and locker activation are here-and-now decisions, while all operational routing, visit, timing, channel, and flow decisions adapt to realized demand scenarios.
- Integrating logistics cost with a service-quality objective that explicitly represents time-window satisfaction, customer walking distance, and delivery charge.
- Providing a reproducible exact–metaheuristic solution framework in which AEC establishes exact reference fronts and a scenario-aware NSGA-II handles large instances through explicit encoding, repair, parameter calibration, convergence analysis, and paired statistical validation.
- Deriving managerial evidence from a 250-customer Tehran case through comparison with an all-direct VRPTW baseline and sensitivity to locker coverage, locker cost, and distance-related cost.

The remainder of the paper is organized as follows. Section 2 reviews the related literature and positions the research gap. Section 3 presents the problem statement and mathematical formulation. Section 4 develops the augmented ε-constraint and NSGA-II solution methods. Section 5 reports computational experiments, statistical comparisons, the case study, sensitivity analysis, and managerial implications. Section 6 concludes the study and identifies limitations and research opportunities.

2- Literature review

The literature is organized into four streams: last-mile and out-of-home delivery, parcel lockers in distribution, pharmaceutical and healthcare logistics, and multi-objective or stochastic vehicle routing. This thematic organization separates the application gap from the methodological gap and supports the comparative synthesis in Section 2.5.

2- 1- Last-mile and out-of-home delivery

Last-mile delivery is frequently the costliest and most environmentally burdensome part of business-to-consumer logistics (Wei et al., 2024). Out-of-home delivery has consequently emerged as a strategy for reducing repeated household stops and improving consolidation (Janinhoff et al., 2024). Pina-Pardo et al. (2022) developed a two-stage last-mile network design model under demand uncertainty, whereas Kim et al. (2024) integrated crowdsourced capacity. Other studies examined loading-zone policies (Muriel et al., 2022), delivery-stop inference from operational data (Basso et al., 2024), autonomous electric vehicles with walking-distance constraints (Moradi et al., 2023), shared collection-and-delivery points (Li et al., 2024), and community time windows (Ouyang et al., 2023). These studies demonstrate the operational value of consolidation but do not address the pharmaceutical combination of cold-chain, returns, and customer-product channel choice.

2- 2- Parcel lockers in distribution

Parcel lockers consolidate several deliveries at accessible self-service locations. Studies report lower last-mile cost and emissions than home delivery under suitable density and utilization conditions (Jiang et al., 2019; Seghezzi et al., 2022; Hovi and Bø, 2024). Research has considered carrier–recipient pricing (Yu et al., 2021), locker placement and accessibility (Zhou et al., 2023; Luo et al., 2022), and routing with lockers. Enthoven et al. (2020) introduced a two-echelon covering VRP; V. F. Yu et al. (2022) modeled simultaneous pickup and delivery with lockers; Dell'Amico et al. (2023) studied pickup and delivery with home-or-locker options; and Vukićević et al. (2023) combined electric vehicles with covering lockers. Mobile-locker models have further introduced learning or recourse under uncertain demand and disruption (Liu et al., 2023; Wang et al., 2024). These contributions establish routing relevance, but customer satisfaction, product heterogeneity, and pharmaceutical safety are generally absent.

2- 3- Pharmaceutical and healthcare logistics

Medicine distribution has distinctive safety, availability, and service requirements. Smart lockers can shorten dispensing queues and improve access for chronic-disease patients (Gobir et al., 2024). Bailey et al. (2013) evaluated locker-box logistics for urgent hospital supplies, Yeo et al. (2021) documented contactless outpatient medication lockers, and Lim et al. (2022) evaluated prescription collection through a locker-box service. For medical supplies more broadly, Shi et al. (2022) formulated a bi-objective drone location-routing problem with simultaneous pickup and delivery. The healthcare literature thus supports locker acceptance and routing relevance, but it does not provide a stochastic home-or-locker VRPTW that explicitly prevents non-refrigerated locker assignment of cold-chain pharmaceuticals.

2- 4- Multi-objective and stochastic vehicle routing

Cost, service quality, and uncertainty make pharmaceutical last-mile distribution inherently multi-objective. Exact ε-constraint variants are effective for mapping efficient solutions in tractable multi-objective mixed-integer models (Mavrotas, 2009; Aghaei et al., 2011), while NSGA-II remains widely used for large combinatorial problems because it combines elitism, non-dominated sorting, and crowding-distance diversity preservation (Deb et al., 2002). Scenario-based two-stage programming separates structural commitments from operational recourse (Pina-Pardo et al., 2022; Wang et al., 2024). The present study combines these methodological threads and validates the metaheuristic against exact results rather than relying on a single algorithm in isolation.

Table 1. Positioning of representative locker-routing and healthcare-logistics studies.

Study	Application	Routing/design feature	Demand uncertainty	Satisfaction objective	Cold-chain rule	Method
Enthoven et al. (2020)	City logistics	Two-echelon covering; cargo bikes and lockers	No	No	No	ALNS
V. F. Yu et al. (2022)	Parcel delivery	Simultaneous pickup/delivery with lockers	No	No	No	Simulated annealing
Dell'Amico et al. (2023)	Parcel delivery	Home-or-locker pickup and delivery	No	No	No	Branch-and-cut
Vukićević et al. (2023)	Green last mile	Electric vehicles and covering lockers	No	No	No	VNS/VND
Liu et al. (2023)	Mobile lockers	Route planning with movable lockers	Limited	No	No	Hybrid Q-learning
Wang et al. (2024)	Mobile lockers	Time windows, pickup and recourse	Yes	No	No	Tabu search
Lim et al. (2022)	Medication collection	Locker-box service evaluation; no VRP	No	Service assessment	No	Empirical study
Shi et al. (2022)	Medical supplies	Drone location-routing; pickup/delivery	No	Bi-objective	No locker	Modified NSGA-II
Zhu et al. (2024)	Locker–drone delivery	Locker-based drone routing	No	No	No	Branch-and-cut
This study	Pharmaceutical last mile	Heterogeneous, multi-product direct/locker VRPTW with returns	Two-stage scenarios	Time, walking, charge	Direct delivery enforced	AEC and NSGA-II

2- 5- Comparative Positioning and Research Gap

Table 1 positions the proposed study against representative routing and healthcare-locker research. The novelty claim is deliberately stated as a joint-feature gap: individual elements exist in prior studies, but their simultaneous treatment in a pharmaceutical two-stage stochastic VRPTW has not been established in the reviewed literature.

The synthesis identifies four connected gaps. First, pharmaceutical locker research is dominated by service evaluation rather than operational route design. Second, locker-routing models rarely combine heterogeneous vehicles, multiple product classes, returns, and customer-product channel decisions. Third, cold-chain feasibility is generally outside the model. Fourth, few studies integrate demand recourse and an explicit customer-satisfaction objective. Section 3 addresses these gaps through a unified formulation, and Sections 4–5 provide exact, heuristic, statistical, and case-based validation.

3- Problem Statement and Mathematical Formulation

This section describes the pharmaceutical distribution problem under study and develops the corresponding bi-objective two-stage stochastic formulation. The distribution system consists of one central distribution center (DC), a set of customers, a set of smart parcel lockers used for indirect delivery, and a heterogeneous fleet of capacitated vehicles. Each customer-product is served through one of two channels: direct door-to-door delivery or indirect delivery to an eligible locker from which the customer collects the parcel. Cold-chain products require direct delivery, whereas ordinary products may use either channel. Deliveries and product returns, including recalled or expired items, are handled within the same vehicle visit.

Each customer specifies a preferred delivery time window. Earliness and lateness in the direct channel are penalized, while locker delivery allows collection after notification and therefore does not incur an earliness penalty. Customer demand is uncertain at the planning stage and is represented by a finite set of discrete scenarios with known probabilities. The company seeks a distribution plan that simultaneously minimizes expected logistics cost and maximizes expected customer satisfaction through on-time service, shorter customer walking distance, and lower shipping charges. Fig. 1 presents the physical structure of the network considered in the model.

3- 1- Modeling assumptions

- Customer demand is uncertain and represented by a finite set S of discrete scenarios. Each scenario s represents one realization of the demand volume and has a known occurrence probability π_s.
- Two delivery channels are available: direct door-to-

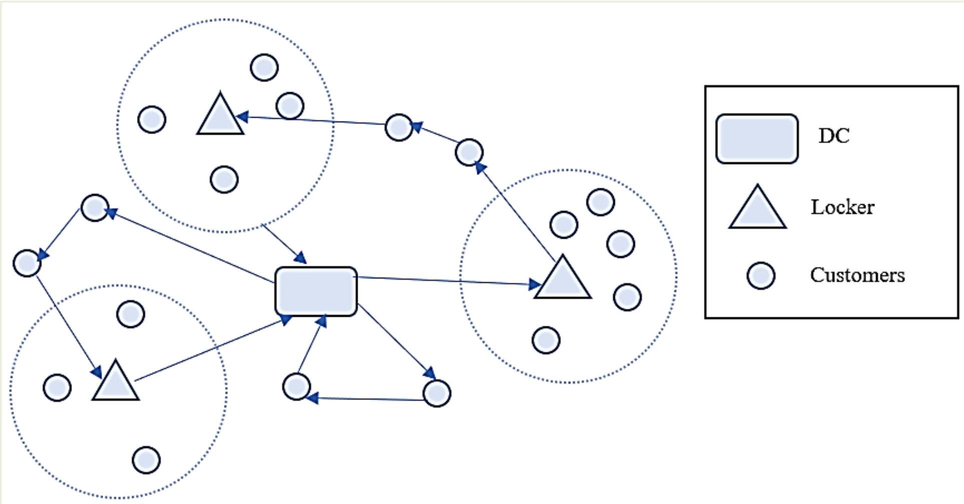

Fig. 1. Schematic representation of the pharmaceutical distribution network (not to scale).

door delivery and indirect locker-based delivery. Each customer specifies a preferred delivery time window when placing an order.

- The product set is partitioned into two mutually exclusive classes, $P = P_c \cup P_n, P_c \cap P_n = \phi$. Cold-chain products in P_c must be delivered directly, whereas ordinary products in P_n may be delivered through either channel.
- Each customer-product is assigned to exactly one service channel, and its demand is not split between channels. A customer may therefore receive different products through different channels, but each customer-product remains unsplit.
- Parcel lockers are not refrigerated and cannot store cold-chain products; consequently, no product in P_c can be assigned to a locker.
- Lockers provide consolidation: in each scenario, at most one vehicle visits an activated locker and the single stop serves all customer-products assigned to that locker. An inactive locker cannot be visited or receive assignments.
- A maximum coverage radius $r^{\max}$ is imposed on locker service. Customer i may be assigned to a locker l only when the eligibility condition represented by a_{il} is satisfied.
- Vehicle capacities Q_k^V and locker capacities Q_l^L are fixed and limited. All product quantities are expressed in compatible capacity units.
- For direct delivery, arrivals before or after the preferred time window incur earliness or lateness penalties. For locker delivery, no earliness penalty is imposed because the customer collects the parcel after notification.
- Product returns are collected only when the customer's address is visited directly; delivery and pickup quantities are transported during the same vehicle visit.
- Only fleet reservation F_k and locker activation u_l are here-and-now decisions made before demand is observed. Vehicle dispatch G_{ks}, route arcs x_{ijks}, node visits v_{iks}, route order ρ_{iks}, service times T_{iks}, channel assignments, product flows, deviations, and realized service quality are wait-and-see decisions that adapt to each scenario s.

3- 2- Two-Stage Stochastic Structure

Two-stage stochastic programming separates decisions according to whether they are made before or after uncertain data are observed. First-stage (here-and-now) decisions are common to all scenarios, whereas second-stage (wait-and-see) decisions can respond to the realized scenario while remaining linked to the first-stage plan. This recourse structure is widely used to connect strategic commitments with adaptive operational decisions under uncertain demand (Hosseini Shekarabi et al., 2026). The generic formulation is given in Eqs. (1)-(2).

Generic two-stage representation

$$\min_{\mathbf{x}\in X}\left\{\mathbf{c}^{\mathsf{T}}\mathbf{x} + \mathbb{E}_{\boldsymbol{\xi}}\left[Q(\mathbf{x},\boldsymbol{\xi})\right]\right\} \tag{1}$$

$$\begin{gathered}\min_{\mathbf{x}\in X}\left\{\mathbf{c}^{\mathsf{T}}\mathbf{x} + \sum_{s\in S}\pi_s\, Q_s(\mathbf{x})\right\}, \\ Q_s(\mathbf{x}) = \min_{\mathbf{y}_s\in Y_s(\mathbf{x})} \mathbf{q}_s^{\mathsf{T}}\mathbf{y}_s\end{gathered} \tag{2}$$

In these relations, $\mathbf{x}$ denotes the generic first-stage decision vector, $\hat{\mathbf{\imath}}$ is the random-data vector, and $Q(\hat{\mathbf{x}},\ )$ is the optimal recourse value. For the finite scenario set S

Table 2. Sets and indices.

Set/index	Definition
V	Set of all nodes: $V = \{0\} \cup V_C \cup V_L$; node 0 is the central DC.
V_C	Set of customers, indexed by i.
V_L	Set of smart parcel lockers, indexed by l.
A	Set of directed feasible arcs (i, j), with i not equal to j.
P	Set of products satisfying $P = P_c \cup P_n$, $P_c \cap P_n = \varnothing$.
P_c	Set of cold-chain (temperature-controlled) products, indexed by p.
P_n	Set of ordinary (non-refrigerated) products, indexed by p.
K	Set of heterogeneous vehicles, indexed by k.
S	Set of demand scenarios, indexed by s.
N	Number of non-depot nodes: $N = \lvert V_C \cup V_L \rvert$.

, $Q_s(\mathbf{x})$ denotes the recourse value under scenario s, and the probabilities satisfy $\pi_s \geq 0, \sum_{s\in S}\pi_s = 1$. In the proposed formulation, the first-stage vector contains only vehicle reservation F_k and locker activation u_l. After scenario s is realized, vehicle dispatch G_{ks}, route selection x_{ijks}, visits v_{iks}, route order ρ_{iks}, service times T_{iks}, channel assignment, commodity flow, direct-service activation, deviations, and realized satisfaction are determined as recourse decisions. The linkage G_{ks} not exceeding F_k prevents a scenario from dispatching a vehicle that was not reserved beforehand.

3- 3- Notation

To avoid symbol overloading, q_{ijkps} is used for multi-product flow and ψ_i denotes the time-satisfaction function. Superscripts identify vehicle, locker, direct-service, earliness, and lateness quantities. Tables 2-5 define every set, parameter, and decision variable used in the formulation.

3- 4- Bi-Objective Stochastic Formulation

3- 4- 1- Objective Functions and Service-Quality Function

The first objective minimizes expected scenario-dependent routing cost, first-stage vehicle-reservation and locker-activation costs, and expected earliness/lateness penalties. The second objective maximizes expected service quality. Coefficients η_T, η_W, η_C place the time-satisfaction, walking-distance, and shipping-charge terms on comparable scales and represent the decision maker's preferences.

Expected-cost components and cost objective

$$C^{\text{route}} = \omega \sum_{s\in S} \pi_s \sum_{k\in K} \sum_{(i,j)\in A} \delta_{ij}\, x_{ijks} \tag{3}$$

$$C^{\text{fixed}} = \sum_{k\in K} c_k^V F_k + \sum_{l\in V_L} c_l^L u_l \tag{4}$$

$$C^{\text{TW}} = \sum_{s\in S} \pi_s \sum_{i\in V_C} \sum_{k\in K} (\lambda_i^E E_{iks} + \lambda_i^L L_{iks}) \tag{5}$$

$$\text{MIN } z_1 = C^{\text{route}} + C^{\text{fixed}} + C^{\text{TW}} \tag{6}$$

Expected service-quality components and satisfaction objective

$$Z^{\text{time}} = \sum_{s\in S} \pi_s \sum_{i\in V_C} \sum_{k\in K} S_{iks} \tag{7}$$

$$Z^{\text{walk}} = \sum_{s\in S} \pi_s \sum_{i\in V_C} \sum_{l\in V_L} \sum_{p\in P_n} \delta_{il}\, y_{ilps} \tag{8}$$

$$Z^{\text{charge}} = \sum_{s\in S} \pi_s \sum_{i\in V_C} \sum_{p\in P} \left(c^D x_{ips}^D + c^L \sum_{l\in V_L} y_{ilps} \right) \tag{9}$$

$$\textbf{MAX } z_2 = \eta_T Z^{\text{time}} - \eta_W Z^{\text{walk}} - \eta_C Z^{\text{charge}} \tag{10}$$

Table 3. Model parameters.

Parameter	Definition
δ_{ij}	Distance associated with directed arc (i,j).
τ_{ij}	Travel time associated with directed arc (i,j).
Q_l^L	Storage capacity of locker l.
Q_k^V	Capacity of vehicle k.
c_l^L	Fixed operating or rental cost of locker l.
c_k^V	First-stage reservation cost of vehicle k.
ω	Transportation cost per unit distance.
c^D, c^L	Shipping charge per customer-product for direct and locker service, respectively.
D_{ips}	Demand of customer i for product p in scenario s.
R_{ip}	Return or pickup quantity of product p at customer i.
e_i, l_i	Lower and upper bounds of customer i's preferred delivery window.
e_i^*, l_i^*	Lower and upper tolerance limits of customer i's satisfaction function.
λ_i^E, λ_i^L	Unit penalties for earliness and lateness at customer i.
φ	Service time per visited node.
$r^{\max}$	Maximum admissible customer-to-locker coverage distance.
a_{il}	Locker-eligibility parameter defined by $a_{il} = 1 \Leftrightarrow \delta_{il} \leq r^{\max}$; 0 otherwise.
π_s	Probability of scenario s, satisfying $\pi_s \geq 0, \quad \sum_{s \in S} \pi_s = 1$.
η_T, η_W, η_C	Nonnegative scaling coefficients for time satisfaction, walking distance, and customer charge.
M	A valid, sufficiently large constant used in conditional constraints.

Table 4. First-stage (here-and-now) decision variables.

Variable	Definition
F_k	1 if vehicle k is reserved before demand is observed; 0 otherwise.
u_l	1 if locker l is activated; 0 otherwise.

Table 5. Second-stage (wait-and-see) decision variables.

Variable	Definition
G_{ks}	1 if reserved vehicle k is dispatched in scenario s; 0 otherwise.
x_{ijks}	1 if vehicle k traverses arc (i,j) in scenario s; 0 otherwise.
v_{iks}	1 if vehicle k visits a non-depot node i in scenario s; 0 otherwise.
ρ_{iks}	MTZ position of non-depot node i in vehicle k's route under scenario s.
T_{iks}	Time at which vehicle k begins service at node i in scenario s.
x^D_{ips}	1 if customer-product (i, p) is assigned to direct service in scenario s; 0 otherwise.
y_{ilps}	1 if ordinary product p of customer i is assigned to locker l in scenario s; 0 otherwise.
w_{is}	1 if customer i receives at least one direct delivery in scenario s; 0 otherwise.
h_{iks}	1 if vehicle k directly serves customer i in scenario s; 0 otherwise.
q_{ijkps}	Quantity of product p carried by vehicle k on arc (i,j) in scenario s.
E_{iks}, L_{iks}	Earliness and lateness of direct service by vehicle k at customer i in scenario s.
S_{iks}	Realized time-window satisfaction of the active direct service, bounded between 0 and 1.

Equations (3)-(6) separately define C^{route}, C^{fixed}, and C^{TW} before assembling the first objective. Equations (7)-(10) similarly define Z^{time}, Z^{walk}, and Z^{charge} before assembling the second objective. Time satisfaction is counted once through the unique active service indicator h_{iks}, rather than once for every vehicle or product.

Trapezoidal time-satisfaction function

$$\psi_i(t) = \begin{cases} 0, & t \le e_i^*, \\ \dfrac{t - e_i^*}{e_i - e_i^*}, & e_i^* < t < e_i, \\ 1, & e_i \le t \le l_i, \\ \dfrac{l_i^* - t}{l_i^* - l_i}, & l_i < t < l_i^*, \\ 0, & t \ge l_i^*, \end{cases} \quad \forall i \in V_C \tag{11}$$

$$h_{iks} = 1 \Rightarrow S_{iks} = \psi_i(T_{iks}),$$
$$h_{iks} = 0 \Rightarrow S_{iks} = 0, \tag{12}$$
$$\forall i \in V_C,\ k \in K,\ s \in S$$

The preferred interval $[e_i, l_i]$ yields full satisfaction. Satisfaction decreases linearly between each preferred bound and its tolerance limit and equals zero outside $[e_i^*, l_i^*]$. Equation (12) activates ψ_i only for the vehicle that directly serves the customer. The bounded piecewise-linear relation is imposed conditionally through the active-service indicator, thereby preserving a consistent linear representation without uncontrolled bilinear products.

3- 4- 2- Scenario-Dependent Routing and Scheduling Constraints

All operational route decisions adapt to the realized scenario. In particular, dispatch G_{ks}, arc use x_{ijks}, node visits v_{iks}, route order ρ_{iks}, and service times T_{iks} carry the scenario index s. The first-stage reservation variable F_k limits scenario-specific dispatch, while locker activation u_l limits visits and assignments to lockers.

Node balance, customer visits, and locker activation

$$\sum_{j \in V} x_{ijks} = \sum_{j \in V} x_{jiks} = v_{iks}, \tag{13}$$
$$\forall i \in V_C \cup V_L,\ k \in K,\ s \in S$$

$$\sum_{k \in K} v_{iks} \le 1, \qquad \forall i \in V_C,\ s \in S \tag{14}$$

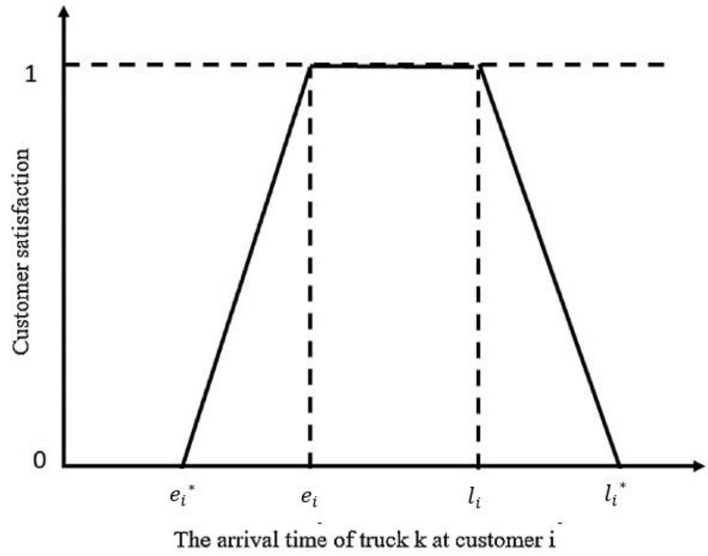

Fig. 2. Trapezoidal customer-satisfaction function for direct-delivery service time.

$$\sum_{k\in K} v_{lks} \le u_l, \qquad \forall l \in V_L,\ s \in S \tag{15}$$

$$y_{ilps} \le \sum_{k\in K} v_{lks}, \quad \forall i \in V_C,\ l \in V_L,\ p \in P_n,\ s \in S \tag{16}$$

Equation (13) equates inbound and outbound degrees at every non-depot node in each scenario and links those degrees to v_{iks}. Equation (14) limits each customer address to at most one vehicle visit per scenario. Equation (15) prohibits visits to inactive lockers and allows at most one vehicle to visit an active locker. Equation (16) requires every locker receiving an assigned customer-product to be visited in the same scenario, thereby preserving route-assignment consistency and the consolidation benefit of locker service.

Depot balance, dispatch, and reservation linkage

$$\sum_{j\in V_C\cup V_L} x_{0jks} = G_{ks}, \qquad \forall k \in K,\ s \in S \tag{17}$$

$$\sum_{i\in V_C\cup V_L} x_{i0ks} = G_{ks}, \qquad \forall k \in K,\ s \in S \tag{18}$$

$$G_{ks} \le F_k, \qquad \forall k \in K,\ s \in S \tag{19}$$

$$x_{ijks} \le G_{ks}, \qquad \forall (i,j) \in A,\ k \in K,\ s \in S \tag{20}$$

Equations (17)-(18) require every dispatched vehicle to leave and return to the DC exactly once in a scenario. Equation (19) is the interstage linking constraint: G_{ks} can equal one only if vehicle k was reserved through F_k before demand was observed. Equation (20) excludes route arcs for vehicles that are not dispatched in the realized scenario.

Subtour elimination and time propagation

$$\rho_{jks} \ge \rho_{iks} + 1 - N\left(1 - x_{ijks}\right), \quad \forall i \ne j \in V_C \cup V_L,\ k \in K,\ s \in S \tag{21}$$

$$v_{iks} \le \rho_{iks} \le N v_{iks}, \quad \forall i \in V_C \cup V_L,\ k \in K,\ s \in S \tag{22}$$

$$T_{jks} \ge T_{iks} + \tau_{ij} + \varphi - M\left(1 - x_{ijks}\right), \quad \forall i \in V,\ j \in V_C \cup V_L,\ k \in K,\ s \in S \tag{23}$$

$$T_{0ks} = 0, \qquad 0 \le T_{iks} \le M v_{iks}, \quad \forall i \in V_C \cup V_L,\ k \in K,\ s \in S \tag{24}$$

Equations (21)-(22) are strengthened scenario-specific MTZ relations. Route positions are positive only at visited nodes and are bounded by N. Equation (23) propagates service start times along every used arc, including travel and service duration. Equation (24) fixes the depot time and deactivates service times at unvisited nodes. Together, these constraints impose a coherent route order and eliminate disconnected cycles in each scenario.

3- 4- 3- Scenario-Dependent Channel Assignment and Service Quality

Exclusive channel assignment

$$x_{ips}^{D} + \sum_{l \in V_L} y_{ilps} = 1, \quad \forall i \in V_C,\ p \in P_n,\ s \in S:\ D_{ips} \neq 0 \tag{25}$$

$$x_{ips}^{D} = 1, \quad \forall i \in V_C,\ p \in P_c,\ s \in S:\ D_{ips} \neq 0 \tag{26}$$

Equation (25) assigns each ordinary customer-product to exactly one channel: direct service or one locker. Equation (26) enforces direct delivery for every cold-chain customer-product, thereby excluding structurally infeasible locker service for refrigerated items.

Direct-service activation and route consistency

$$x_{ips}^{D} \leq w_{is}, \qquad \forall i \in V_C,\ p \in P,\ s \in S \tag{27}$$

$$w_{is} \leq \sum_{p \in P} x_{ips}^{D}, \qquad \forall i \in V_C,\ s \in S \tag{28}$$

$$x_{ips}^{D} \leq \sum_{k \in K} v_{iks}, \qquad \forall i \in V_C,\ p \in P,\ s \in S \tag{29}$$

Equations (27)-(28) define w_{is} exactly: it equals one if and only if at least one product of customer i is delivered directly in scenario s. Equation (29) permits direct assignment only when that customer's address is visited in the same scenario.

Locker availability and coverage

$$y_{ilps} \leq u_l, \qquad \forall i \in V_C,\ l \in V_L,\ p \in P_n,\ s \in S \tag{30}$$

$$y_{ilps} \leq a_{il}, \qquad \forall i \in V_C,\ l \in V_L,\ p \in P_n,\ s \in S \tag{31}$$

Equation (30) allows assignment only to a locker activated in the first stage. Equation (31) uses the precomputed binary parameter a_{il} to remove assignments beyond the maximum coverage radius $r^{\max}$.

Vehicle-specific direct service and time deviations

$$\sum_{k \in K} h_{iks} = w_{is}, \qquad \forall i \in V_C,\ s \in S \tag{32}$$

$$h_{iks} \leq v_{iks}, \qquad \forall i \in V_C,\ k \in K,\ s \in S \tag{33}$$

$$E_{iks} \geq e_i - T_{iks} - M(1 - h_{iks}), \quad \forall i \in V_C,\ k \in K,\ s \in S \tag{34}$$

$$L_{iks} \geq T_{iks} - l_i - M(1 - h_{iks}), \quad \forall i \in V_C,\ k \in K,\ s \in S \tag{35}$$

$$0 \leq E_{iks} \leq M h_{iks}, \quad \forall i \in V_C,\ k \in K,\ s \in S \tag{36}$$

$$0 \leq L_{iks} \leq M h_{iks}, \quad \forall i \in V_C,\ k \in K,\ s \in S \tag{37}$$

Equations (32)-(33) select the unique routed vehicle that performs direct service in each scenario. This vehicle-specific activation prevents earliness and lateness penalties from being applied to nonvisiting vehicles. Equations (34)-(37) define the nonnegative deviations E_{iks} and L_{iks} and force both to zero whenever h_{iks}=0.

3- 4- 4- Capacity and multi-product flow conservation

Locker and vehicle capacities

$$\sum_{i \in V_C} \sum_{p \in P_n} D_{ips}\, y_{ilps} \leq Q_l^{L} u_l, \quad \forall l \in V_L,\ s \in S \tag{38}$$

$$\sum_{p \in P} q_{ijkps} \leq Q_k^{V} x_{ijks}, \quad \forall (i,j) \in A,\ k \in K,\ s \in S \tag{39}$$

Equation (38) limits the consolidated demand allocated to each activated locker in every scenario. Equation (39) links the multi-product flow on each arc to the scenario-indexed route variable x_{ijks} and enforces heterogeneous vehicle capacity for the same scenario.

Depot dispatch and return balance

$$\sum_{k\in K}\sum_{j\in V_C\cup V_L} q_{0jkps} = \sum_{i\in V_C} D_{ips}, \quad \forall p \in P,\ s \in S \tag{40}$$

$$\sum_{k\in K}\sum_{j\in V_C\cup V_L} q_{j0kps} = \sum_{i\in V_C} R_{ip}\, w_{is}, \quad \forall p \in P,\ s \in S \tag{41}$$

Equation (40) dispatches the full demand of every product from the DC. Equation (41) returns only the pickup quantities associated with customers whose addresses are visited directly. The factor w_{is} maintains consistency with the customer-node balance and with the assumption that returns are collected during direct service.

Customer and locker flow balance

$$\sum_{k\in K}\left(\sum_{j\in V} q_{jikps} - \sum_{j\in V} q_{ijkps}\right) = D_{ips}x^{D}_{ips} - R_{ip}w_{is}, \quad \forall i \in V_C,\ p \in P,\ s \in S \tag{42}$$

$$\sum_{k\in K}\left(\sum_{j\in V} q_{jlkps} - \sum_{j\in V} q_{ljkps}\right) = \sum_{i\in V_C} D_{ips}\, y_{ilps}, \quad \forall l \in V_L,\ p \in P_n,\ s \in S \tag{43}$$

Equation (42) states that net product inflow at a customer equals its direct delivery minus the return collected during a direct visit. Equation (43) states that net inflow at a locker equals the consolidated ordinary-product demand assigned to that locker. The symbol q_{ijkps} is used consistently for commodity flow to avoid conflict with ψ_i.

3- 4- 5- Variable Domains

$$F_k,\ u_l \in \{0,1\} \tag{44}$$

$$G_{ks},\ x_{ijks},\ v_{iks} \in \{0,1\} \tag{45}$$

$$x^{D}_{ips},\ y_{ilps},\ w_{is},\ h_{iks} \in \{0,1\} \tag{46}$$

$$q_{ijkps},\ T_{iks},\ \rho_{iks},\ E_{iks},\ L_{iks} \ge 0,\quad 0 \le S_{iks} \le 1 \tag{47}$$

Equation (44) contains the only first-stage variable domains: vehicle reservation F_k and locker activation u_l. Equations (45)-(47) specify the scenario-dependent binary and continuous recourse domains. The MTZ variables ρ_{iks} may remain continuous because integrality of x_{ijks} is sufficient to impose the route order. The bounds on S_{iks} preserve its interpretation as a normalized satisfaction score.

The resulting formulation is a bi-objective two-stage stochastic mixed-integer model that integrates direct home delivery, locker-based service, time-window satisfaction, vehicle and locker capacities, returns, and multi-product flow conservation. Its here-and-now layer contains only vehicle reservation F_k and locker activation u_l. After demand is observed, dispatch G_{ks}, routing x_{ijks}, visits v_{iks}, route order ρ_{iks}, service times T_{iks}, assignments, flows, and service-quality variables adapt to each scenario while remaining linked to the reserved fleet and activated lockers. Expected costs and service measures are weighted by scenario probabilities, and direct-service penalties are evaluated only for the vehicle that actually serves the customer. In Section 4, exact and metaheuristic solution approaches are developed to solve the proposed bi-objective optimization model.

4- Solution Approach

The proposed formulation is a bi-objective two-stage stochastic mixed-integer program. A single optimum cannot represent the trade-off between total logistics cost and customer satisfaction; the solution process must therefore approximate or enumerate a Pareto set. For small and medium instances, the augmented ε-constraint (AEC) method supplies exact efficient solutions and a reference front. For larger instances, a scenario-aware non-dominated sorting genetic algorithm (NSGA-II) provides scalable search. The methods are complementary: AEC establishes optimality-based benchmarks, whereas NSGA-II targets computational tractability and diversity.

4- 1- Augmented ε-Constraint Method

Because the second objective is maximized, the bi-objective model is written in minimization form through $\mathbf{f}$ with components z_1 and the negative of z_2, as shown in Eq. (48). The feasible region Ω is defined by Eqs. (3)–(47), including the first-stage and recourse domains.

Bi-objective representation

$$\min_{\mathbf{x}\in\Omega} \mathbf{f}(\mathbf{x}) = \left(f_1(\mathbf{x}), f_2(\mathbf{x})\right) = \left(z_1(\mathbf{x}), -z_2(\mathbf{x})\right) \tag{48}$$

The payoff table is constructed lexicographically rather than by solving each objective in isolation. Equation (49) obtains the cost anchor $\mathbf{x}^{(1)}$ and the satisfaction anchor $\mathbf{x}^{(2)}$, with the secondary objective breaking ties. Equation (50) then defines the attainable satisfaction interval and its range r_2. Lexicographic anchors prevent an arbitrary weakly efficient endpoint from distorting the ε-grid (Mavrotas, 2009; Aghaei et al., 2011; Razavi Al-e-hashem et al., 2022).

Lexicographic anchors and normalization range

$$\begin{aligned} \mathbf{x}^{(1)} &= \operatorname*{lexmin}_{\mathbf{x}\in\Omega}(z_1, -z_2), \\ \mathbf{x}^{(2)} &= \operatorname*{lexmin}_{\mathbf{x}\in\Omega}(-z_2, z_1) \end{aligned} \tag{49}$$

$$\begin{aligned} z_2^{\min} &= z_2\left(\mathbf{x}^{(1)}\right), \\ z_2^{\max} &= z_2\left(\mathbf{x}^{(2)}\right), \\ r_2 &= z_2^{\max} - z_2^{\min} \end{aligned} \tag{50}$$

The interval is divided into q equal subintervals. At grid point e_ℓ, the satisfaction objective is moved to the constraint set. The nonnegative slack s_ℓ measures satisfaction above the imposed bound. A small positive ε rewards slack after scaling by r_2, eliminating weakly efficient solutions without changing the priority assigned to cost.

AEC grid and augmented subproblem

$$e_\ell = z_2^{\min} + \frac{\ell}{q}\left(z_2^{\max} - z_2^{\min}\right), \qquad \ell = 0,1,\dots,q \tag{51}$$

$$\begin{aligned} &\min_{\mathbf{x},s_\ell} \left\{z_1(\mathbf{x}) - \varepsilon\frac{s_\ell}{r_2}\right\} \quad \text{s.t.} \\ &z_2(\mathbf{x}) - s_\ell = e_\ell,\; s_\ell \geq 0,\; \mathbf{x}\in\Omega \end{aligned} \tag{52}$$

Each feasible grid subproblem is solved to prove optimality in the exact implementation. Duplicate objective pairs are removed, and a final non-dominance filter produces $\mathcal{P}^{\mathrm{AEC}}$ in Eq. (53). Infeasible grid values are skipped; thus the procedure remains valid even when portions of the nominal objective range are disconnected.

Exact efficient set

$$\mathcal{P}^{\mathrm{AEC}} = \mathrm{ND}\left\{\left(z_1(\mathbf{x}_\ell), z_2(\mathbf{x}_\ell)\right) : \ell = 0,\dots,q\right\} \tag{53}$$

The exact models are implemented in GAMS. The payoff-table solves, the grid subproblems, and the final dominance check are executed in the order summarized in Fig. 3. Since each grid point requires a mixed-integer solve, runtime grows rapidly with the number of customers, lockers, products, scenarios, and grid points; this motivates the metaheuristic for large instances.

4- 2- Scenario-Aware NSGA-II

NSGA-II is an elitist population-based multi-objective algorithm that uses fast non-dominated sorting for convergence and crowding distance for diversity (Deb et al., 2002). It is particularly suitable here because permutation and categorical genes can directly represent routes and delivery channels, while a problem-specific decoder and repair operator enforce the complex pharmaceutical constraints. Fig. 4 summarizes the full evolutionary cycle.

4- 2- 1- Solution Representation and Nonanticipativity

A chromosome contains one shared first-stage block and one recourse block for every scenario. The shared block records reserved vehicles F_k and activated lockers u_l. Within scenario s, the recourse block contains: (i) a priority sequence of customer and locker nodes separated by vehicle delimiters and decoded into G_{ks}, x_{ijks}, v_{iks}, ρ_{iks}, and T_{iks}; and (ii) a channel gene for each customer-product, where zero represents direct service and a positive eligible locker identifier represents indirect service. Fig. 5 illustrates one recourse block; the same structure is repeated for each scenario while the first-stage block is stored only once. This architecture enforces nonanticipativity by construction.

4- 2- 2- Initialization and Feasibility-Preserving Decoding

Initial chromosomes are generated randomly within feasibility-oriented rules. Cold-chain products are assigned directly; ordinary products are sampled from direct delivery or eligible activated lockers; locker capacity is checked before acceptance; and all directly served customers and visited lockers are inserted into vehicle sequences. The decoder then constructs depot-to-depot routes, assigns quantities, propagates service times, and evaluates both objectives with scenario probabilities. A first-stage vehicle or locker is activated whenever at least one recourse block requires it, so the fixed-cost envelope is the minimum shared commitment supporting all scenarios.

4- 2- 3- Non-Dominated Sorting, Crowding, and Selection

For consistent comparison, the objective vector is $\mathbf{f} = \left(z_1, -z_2\right)$. Equation (54) defines Pareto dominance. Individuals with domination count zero form the first front; removing them recursively produces subsequent fronts. Within each front, the boundary solutions receive infinite crowding distance, and each interior distance is computed by Eq. (55) after objective-wise normalization. Binary

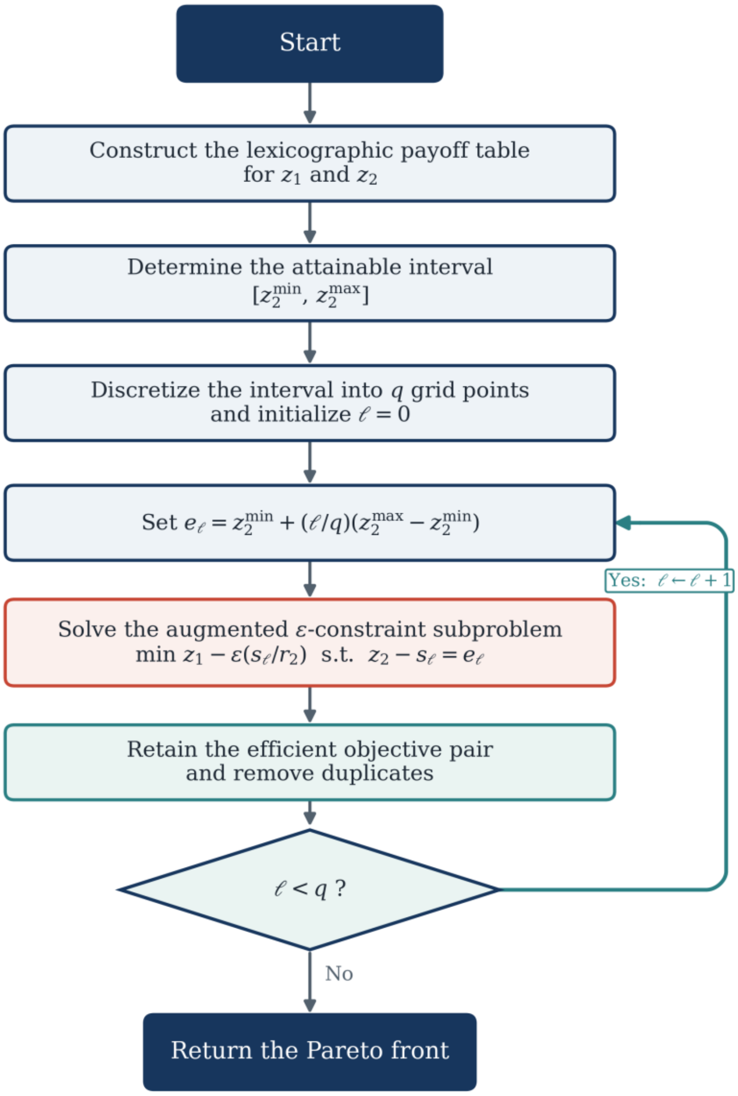

Fig. 3. Flowchart of the augmented ε-constraint (AEC) procedure.

tournament selection follows Eq. (56): lower rank is preferred, and crowding distance breaks rank ties.

Dominance, crowding distance, and tournament order

$$\mathbf{a} \prec \mathbf{b} \Leftrightarrow [\forall m:\ f_m(\mathbf{a}) \le f_m(\mathbf{b})] \wedge \left[\exists m:\ f_m(\mathbf{a}) < f_m(\mathbf{b})\right] \tag{54}$$

$$CD_i = \sum_{m=1}^{M_o} \frac{f_{m,i+1} - f_{m,i-1}}{f_m^{\max} - f_m^{\min}} \tag{55}$$

$$\mathbf{a} \succ_T \mathbf{b} \Leftrightarrow (r_a < r_b) \vee (r_a = r_b\ \wedge\ CD_a > CD_b) \tag{56}$$

4- 2- 4- Genetic Operators and Repair

Uniform crossover and bit-flip mutation operate on the shared reservation and activation block. Ordered crossover preserves relative node order in routing blocks, while uniform crossover recombines channel genes. Swap and insertion mutations diversify routes, and an assignment mutation selects an alternative eligible channel. After recombination, repair proceeds in a fixed order: cold-chain correction; locker eligibility and capacity correction; removal of duplicate or unserved nodes; vehicle-capacity rebalancing; route resequencing; and time-feasibility improvement. If a locker assignment changes, its visit status is updated in the same scenario. This joint repair prevents the route–assignment inconsistency that would otherwise undermine consolidation.

4- 2- 5- Elitist Replacement and Termination

At generation G, parent population P_g and offspring

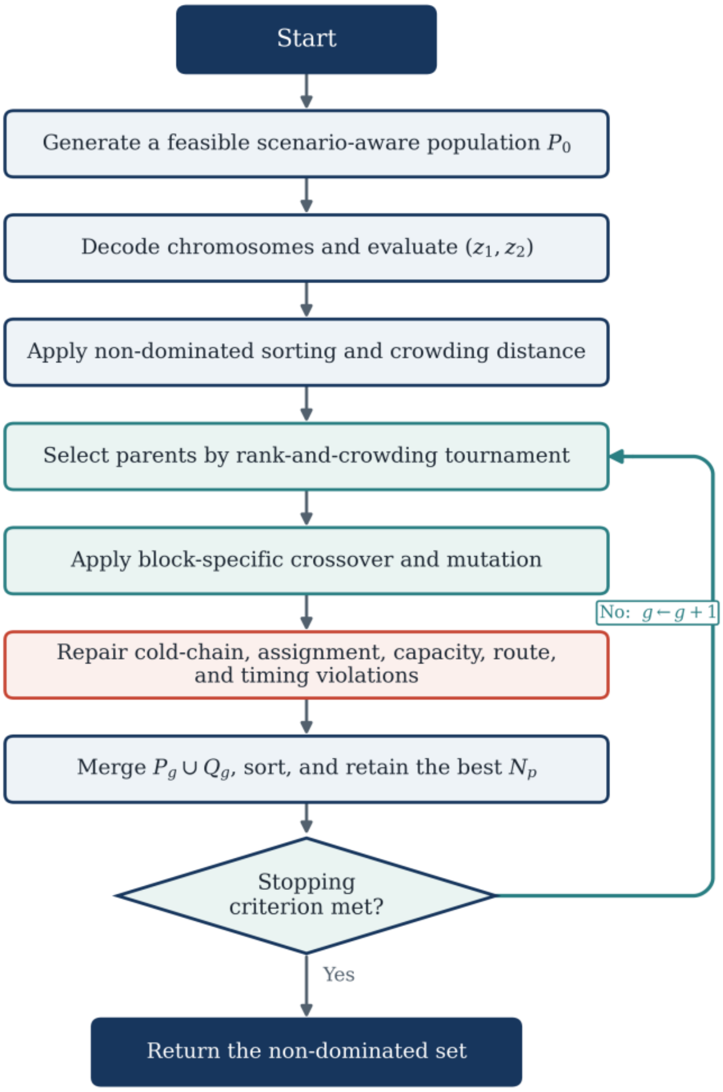

Fig. 4. Flowchart of the proposed scenario-aware NSGA-II.

population Q_g are merged. Equation (57) retains the best N_p individuals by successive fronts; if the final accepted front does not fit completely, the individuals with the largest crowding distances are selected. The algorithm terminates after the calibrated generation limit, and the non-dominated members of the final population are returned.

Elitist population update

$$R_g = P_g \cup Q_g, \qquad P_{g+1} = \mathrm{Select}_{N_p}\left(R_g;\ r, CD\right) \tag{57}$$

4- 2- 6- Parameter Calibration and Convergence Criterion

Four control parameters were calibrated at three levels using a Taguchi design. For a smaller-is-better performance response d_r, Eq. (58) converts replicated outcomes into a larger-is-better S/N measure. Table 6 reports the tested levels and selected configuration. The convergence record uses the normalized gap in Eq. (59), where the reference is the best available exact or incumbent value for the representative instance.

Taguchi signal-to-noise ratio and convergence gap

$$\mathrm{S/N} = -10\log_{10}\left(\frac{1}{R}\sum_{r=1}^{R} d_r^2\right) \tag{58}$$

$$\mathrm{gap}_g = \frac{\left|z_1^{\mathrm{best}}(g) - z_1^{\mathrm{ref}}\right|}{\max\{1, \left|z_1^{\mathrm{ref}}\right|\}} \tag{59}$$

The larger-is-better main effects select a population

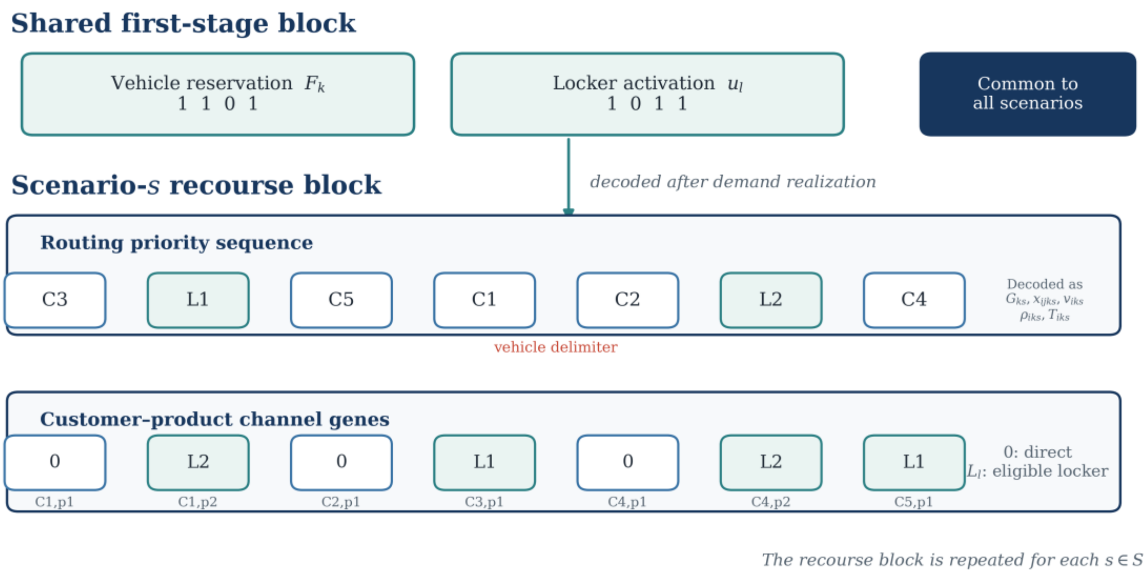

Fig. 5. Shared first-stage and scenario-dependent chromosome architecture used in NSGA-II.

Algorithm 1. Proposed scenario-aware NSGA-II.

1: Generate N_p feasible chromosomes with a shared first-stage block and scenario-specific recourse blocks.

2: Decode every chromosome; evaluate expected z_1 and z_2.

3: Apply fast non-dominated sorting and crowding-distance assignment.

4: While the stopping criterion is not met, repeat Steps 5–12.

5: Select parents by rank-and-crowding binary tournament.

6: Apply block-specific crossover to reservation, routing, and channel genes.

7: Apply bit-flip, swap, insertion, and eligible-channel mutations.

8: Repair cold-chain, coverage, locker-capacity, vehicle-capacity, routing, and timing violations.

9: Decode and evaluate offspring population Q_g.

10: Form combined population $R_g = P_g \cup Q_g$.

11: Sort R_g and select the best N_p individuals using rank and CD.

12: Update the generation counter and convergence record.

13: Return the final non-dominated set.

Table 6. NSGA-II control-parameter levels and selected values.

Parameter	Level 1	Level 2	Level 3	Selected value
Population size	100	150	200	200
Generations	250	500	750	500
Crossover rate	0.60	0.70	0.80	0.70
Mutation rate	0.10	0.25	0.40	0.25

Fig. 6. Main-effects plots for the Taguchi signal-to-noise ratios.

of 200, 500 generations, crossover probability 0.70, and mutation probability 0.25. Fig. 7 shows that the representative first-objective gap drops below 0.002 at generation 135 and remains stable. The 500-generation limit therefore provides a substantial post-convergence buffer for the reported experiments.

5- Computational Results, Case Study, and Managerial Analysis

This section reports the experimental design, exact and metaheuristic results, paired statistical validation, the Tehran case study, baseline comparison, and sensitivity analysis. Cost values are reported in monetary units (MU) because the confidential case dataset does not identify a publication currency. The second objective is a dimensionless aggregate customer-satisfaction index; higher values are preferred. Runtime is reported in seconds. This explicit labeling avoids interpreting the two objectives as directly commensurate quantities.

5- 1- Experimental Design and Demand Scenarios

The case application is based on pharmaceutical distribution operations of Alborz Distribution Company in Tehran. The available computational record contains

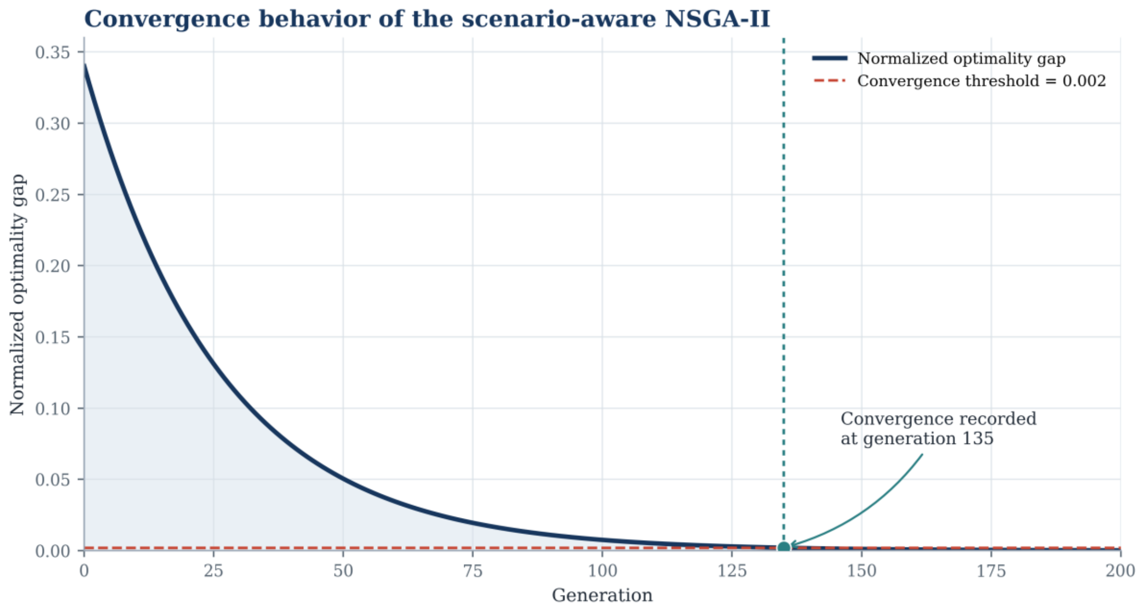

Fig. 7. Convergence of NSGA-II for a representative first-objective run.

Table 7. Demand scenarios and probability calibration.

Scenario	Demand uplift (%)	Probability	Weighted contribution (percentage points)
S1	10	0.25	2.50
S2	15	0.42	6.30
S3	20	0.33	6.60
Total / mean	—	1.00	15.40

customer, candidate-locker, product, vehicle-type, and fleet-size information. Demand uncertainty is represented by three discrete uplift scenarios derived from the demand bands observed in the five-year record. A scenario representation is appropriate because the reported demand pattern did not conform to a standard parametric distribution; it also permits direct control of high-demand feasibility through scenario-specific recourse (Wets, 1994; Arabatzis et al., 2013).

The probability-weighted mean uplift is $\mu_{\Delta} = 15.4\%$, and the probability-weighted standard deviation is $\sigma_{\Delta} = 3.79$ percentage points. Thus the scenario support spans a 10-percentage-point demand band around a moderate central uplift. Rather than fixing one route across that band, the two-stage model maintains common reservation and activation decisions while allowing dispatch, routes, visits, times, assignments, and flows to adapt. The numerical results below are probability-weighted outputs over this scenario set.

5- 2- Exact AEC Benchmark Results

Table 8 reports representative efficient solutions obtained by the exact AEC implementation in GAMS. Instance size grows jointly in customers, lockers, products, vehicle types, and available vehicles. Exact runtime rises from 5 s for the smallest instance to 68 s for the fifth instance, illustrating the increasing burden of repeated mixed-integer subproblems.

Both objective values increase with instance scale because the cost objective aggregates more deliveries and the satisfaction objective aggregates service across more customer-product requests. These values are therefore used as within-instance solution criteria, not as normalized cross-instance performance measures.

5- 3- NSGA-II Computational Performance

Table 9 reports NSGA-II results for the same five instance sizes. The metaheuristic requires 1–17 s, compared with 5–68 s for AEC. Because each row represents one selected efficient

Table 8. Exact AEC results for small and medium benchmark instances.

Inst.	Customers	Lockers	Products	Vehicle types	Vehicles	Cost z_1 (MU)	Satisfaction z_2	Runtime (s)
1	3	1	2	1	2	3,969	812	5
2	5	3	4	2	2	5,160	1,263	32
3	10	5	8	3	3	9,565	1,797	39
4	15	10	12	4	4	13,189	2,091	56
5	20	15	15	4	6	19,852	2,842	68

Table 9. NSGA-II results for the five common benchmark instances.

Instance	Cost z_1 (MU)	Satisfaction z_2	Runtime (s)
1	4,612	520	1
2	6,413	857	6
3	11,200	1,074	11
4	21,329	1,365	14
5	27,643	2,058	17

solution rather than an identical ε-level, the objective values should not be compared row-by-row as if they were single-objective optima; the Pareto-set indicators in Section 5.4 provide the appropriate quality comparison.

AEC requires 200 s in total across the five instances, whereas NSGA-II requires 49 s, corresponding to an aggregate speedup of 4.08. The mean runtimes are 40.0±24.14 s and 9.8±6.38 s, respectively. A one-sided paired Wilcoxon signed-rank test confirms lower NSGA-II runtime at the 5% level ($p=0.0313$). The runtime advantage becomes operationally relevant as the exact grid and mixed-integer tree expand.

5- 4- Pareto-Set Quality and Paired Statistical Validation

Three indicators evaluate the 15 paired benchmark fronts. The two objectives are first transformed to common minimization directions and scaled relative to the ideal and nadir values by Eq. (60). NPS in Eq. (61) counts non-dominated solutions and is maximized. MID in Eq. (62) measures average normalized distance to the ideal point and is minimized. SM in Eq. (63) measures dispersion of consecutive front distances and is minimized (Rabiei et al., 2023; Zitzler et al., 2000).

Normalized Pareto quality indicators

$$\hat{z}_1 = \frac{z_1 - z_1^*}{z_1^{\mathrm{nad}} - z_1^*}, \qquad \hat{z}_2 = \frac{z_2^* - z_2}{z_2^* - z_2^{\mathrm{nad}}} \tag{60}$$

$$\mathrm{NPS} = |\mathcal{P}^{\mathrm{ND}}| \tag{61}$$

$$\mathrm{MID} = \frac{1}{n}\sum_{r=1}^{n}\sqrt{\hat{z}_{1r}^{\,2} + \hat{z}_{2r}^{\,2}} \tag{62}$$

$$\mathrm{SM} = \frac{\sum_{r=1}^{n-1}|d_r - \bar{d}|}{(n-1)\bar{d}} \tag{63}$$

The results reveal a transparent trade-off between exactness and diversity. NSGA-II returns significantly more non-dominated alternatives and is faster, while AEC retains a significantly better average distance to the ideal point. The methods have statistically indistinguishable spacing. Consequently, AEC is preferable when exact proximity is paramount, and instance size is manageable; NSGA-II is preferable when decision makers need a broad front quickly for large networks.

5- 5- Tehran Pharmaceutical-Distribution Case Study

The large case represents pharmaceutical distribution in Tehran by Alborz Distribution Company. It contains 250 customer locations, 162 candidate lockers, 30 product types, four vehicle types, and 20 vehicles. Fig. 11 shows the geographic network. The map retains the customer and

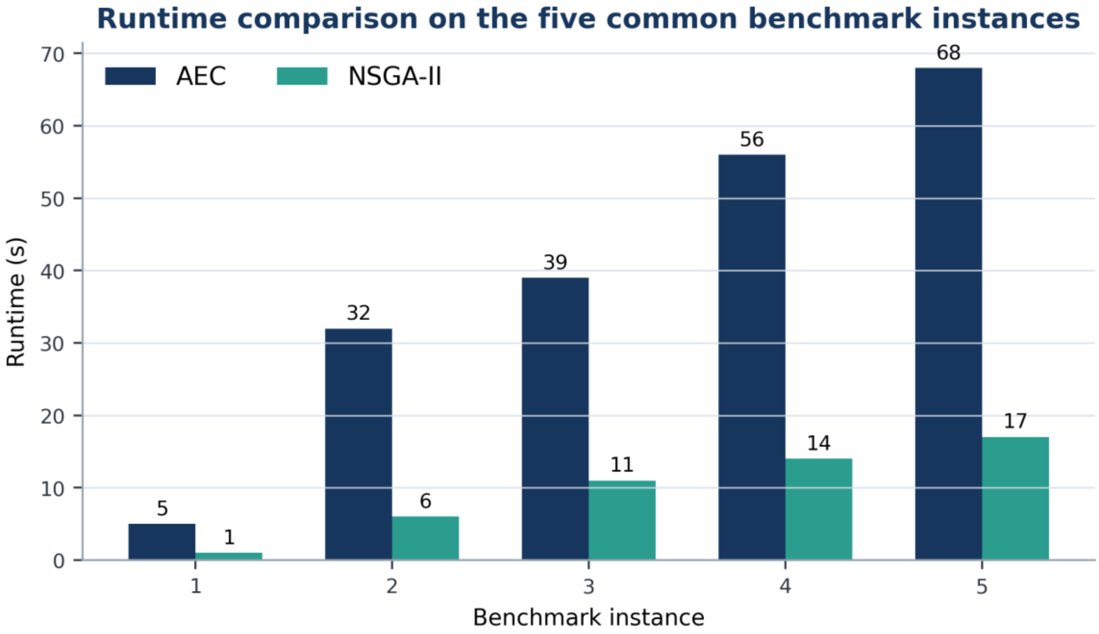

Fig. 8. Runtime comparison between AEC and NSGA-II on common benchmark instances.

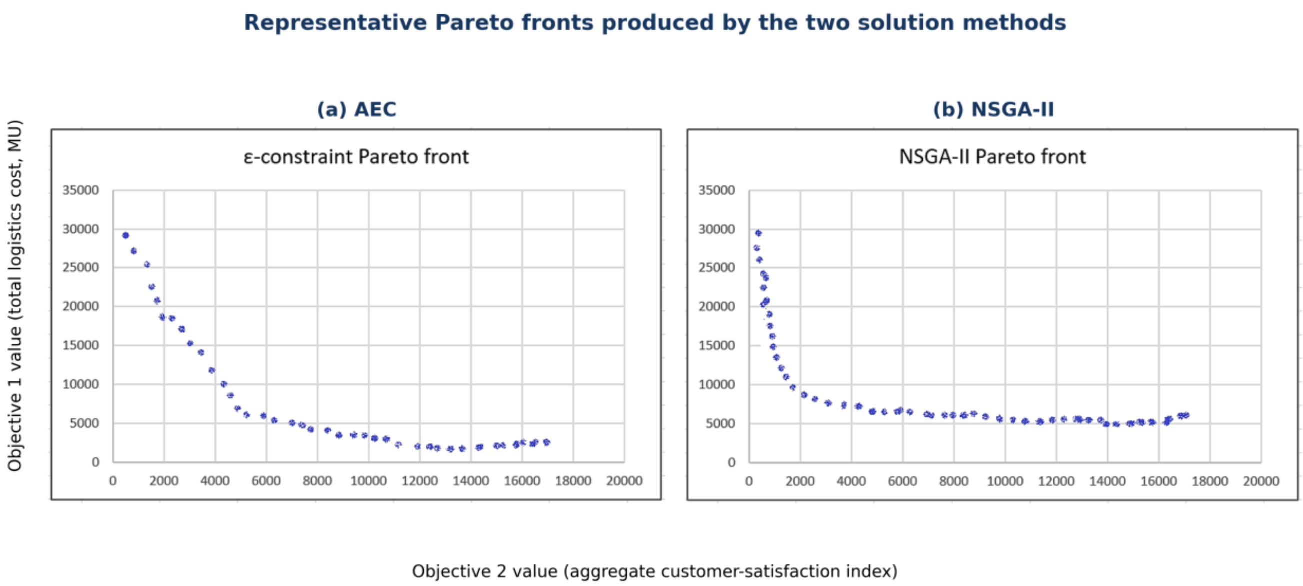

Fig. 9. Representative Pareto fronts produced by AEC and NSGA-II; lower cost and higher satisfaction are preferred.

Table 10. Pareto quality indicators on 15 paired benchmark instances.

Inst.	AEC NPS	AEC MID	AEC SM	NSGA-II NPS	NSGA-II MID	NSGA-II SM
1	10	1.100	0.61	16	1.600	0.71
2	9	1.400	0.73	20	1.400	0.84
3	11	1.000	0.83	22	1.300	0.43
4	16	1.350	0.54	25	1.600	0.73
5	23	1.120	0.92	17	1.400	0.53
6	15	1.650	0.74	19	1.300	0.42
7	8	1.010	0.65	11	1.000	0.61
8	13	1.080	0.81	26	1.430	0.71
9	20	1.023	0.95	28	1.000	0.74
10	18	1.500	0.66	27	1.200	0.73
11	17	1.300	0.45	18	1.710	0.62
12	22	1.000	0.76	19	1.470	0.74
13	21	1.400	0.23	29	1.870	0.41
14	18	1.380	0.45	23	1.430	0.61
15	17	1.400	0.62	20	1.500	0.48

locker legend from the original case record; candidate sites are evaluated jointly with routing and service decisions.

The selected compromise solution has a total cost of 74,559 MU and an aggregate satisfaction value of 27,923, obtained in 28 s. The complete front in Fig. 12 allows a decision maker to choose a different cost–service compromise without rerunning the algorithm. Because the case is substantially larger than the exact benchmark set, it also demonstrates the operational role of the metaheuristic.

5- 6- Baseline Comparison: Mixed Delivery Versus All-Direct VRPTW

To establish an interpretable baseline, the proposed mixed direct–locker strategy is compared with a classical all-direct pharmaceutical VRPTW in which locker assignment is disabled. Table 13 decomposes both objectives. For satisfaction, the model maximizes the time-window score and subtracts walking-distance and delivery-charge penalties; the walking component therefore becomes zero in the all-direct policy, but this isolated benefit is outweighed by poorer time performance and higher delivery charge.

Removing lockers saves 3,724 MU in activation cost but increases time-window penalties, distance cost, and fleet cost. The net result is an 8,201 MU increase, equivalent to 11.0%. The all-direct policy removes customer walking, yet its lower time-window score and higher delivery-charge penalty reduce total satisfaction by 3,676 points, or 13.17%. The proposed strategy therefore dominates the operational baseline on both reported objectives.

5- 7- Sensitivity and Robustness Analysis

5- 7- 1- Locker-Cost and Distance-Cost Stress Tests

Reviewer-requested cost sensitivities are derived directly from the reported case components without inventing re-optimization outcomes. Let α_L multiply the locker cost and β_D multiply the distance-related transport cost, holding the selected routes and all other components fixed. Equations (64)–(65) define the resulting ceteris paribus totals. The mixed strategy remains cheaper than all-direct delivery until the locker-cost multiplier reaches $\alpha_L^{\mathrm{BE}} = 3.202$, i.e., a 220.2% increase above its baseline value.

Post-optimal cost functions

$$C_{\mathrm{mix}}(\alpha_L) = 70835 + 3724\alpha_L, \quad C_{\mathrm{direct}} = 82760, \quad \alpha_L^{\mathrm{BE}} = 3.202 \tag{64}$$

$$C_{\mathrm{mix}}(\beta_D) = 50630 + 23929\beta_D, \quad C_{\mathrm{direct}}(\beta_D) = 55720 + 27040\beta_D \tag{65}$$

The distance-cost stress test also favors consolidation:

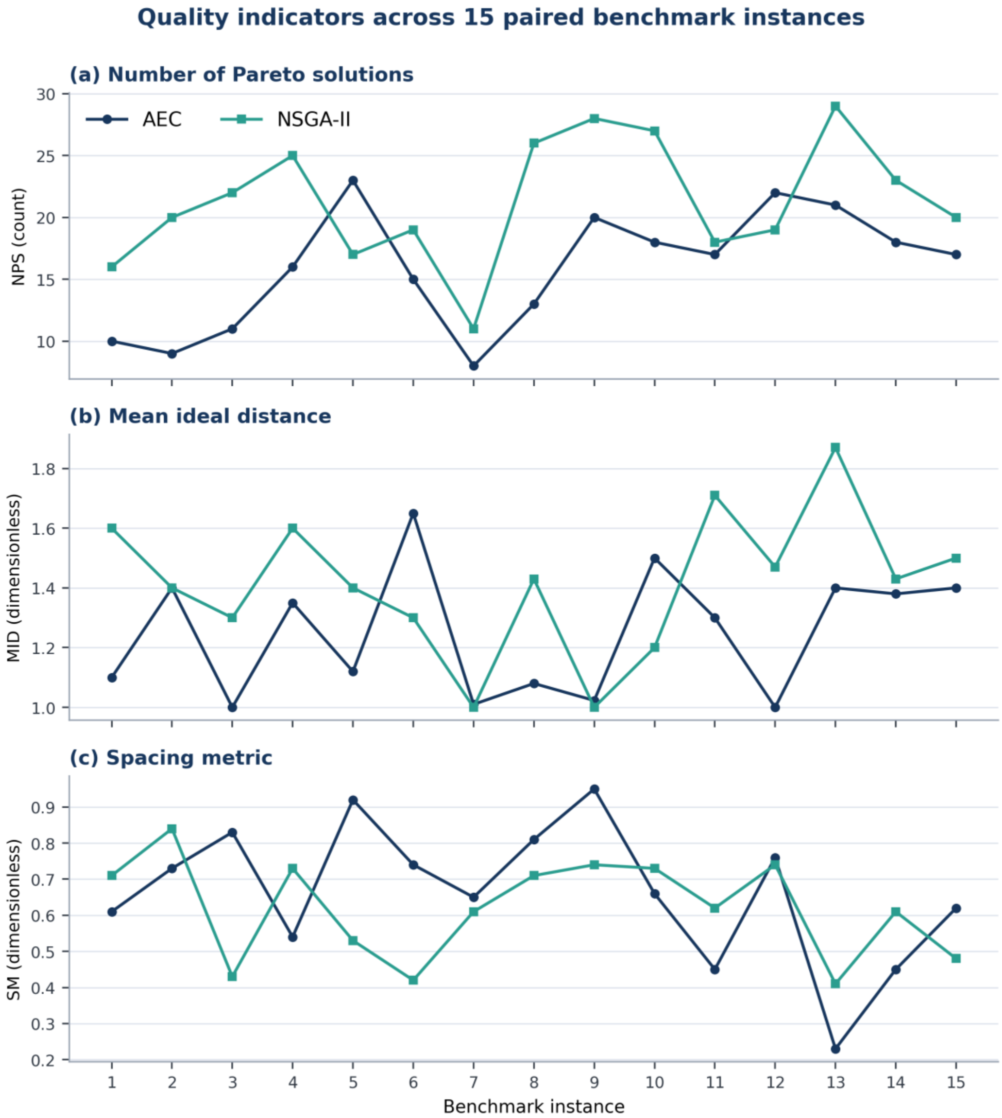

Fig. 10. NPS, MID, and SM values for the 15 paired benchmark instances.

Table 11. Summary statistics and paired Wilcoxon tests for Pareto quality.

Metric	Preferred direction	AEC mean±SD	NSGA-II mean±SD	Relative NSGA-II change	Two-sided p-value	Interpretation
NPS	Higher	15.87±4.78	21.33±5.02	+34.45%	0.0049	NSGA-II yields significantly more non-dominated solutions
MID	Lower	1.248±0.211	1.414±0.238	+13.34%	0.0412	AEC is significantly closer to the ideal point
SM	Lower	0.663±0.192	0.621±0.138	−6.43%	0.6387	Spacing difference is not statistically significant

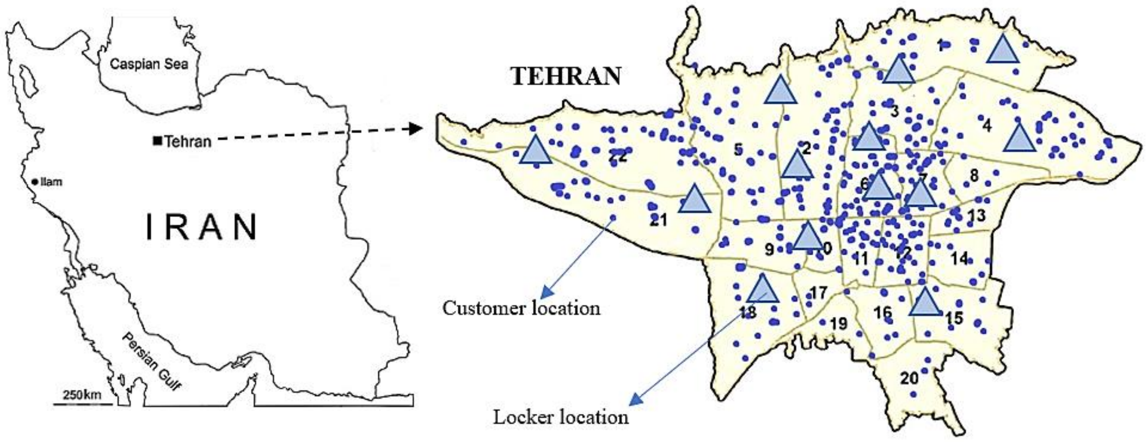

Fig. 11. Geographic distribution of customers and candidate lockers in the Tehran case study.

Table 12. Case-study dimensions and selected NSGA-II solution.

Customers	Candidate lockers	Products	Vehicle types	Vehicles	Cost z_1 (MU)	Satisfaction z_2	Runtime (s)
250	162	30	4	20	74,559	27,923	28

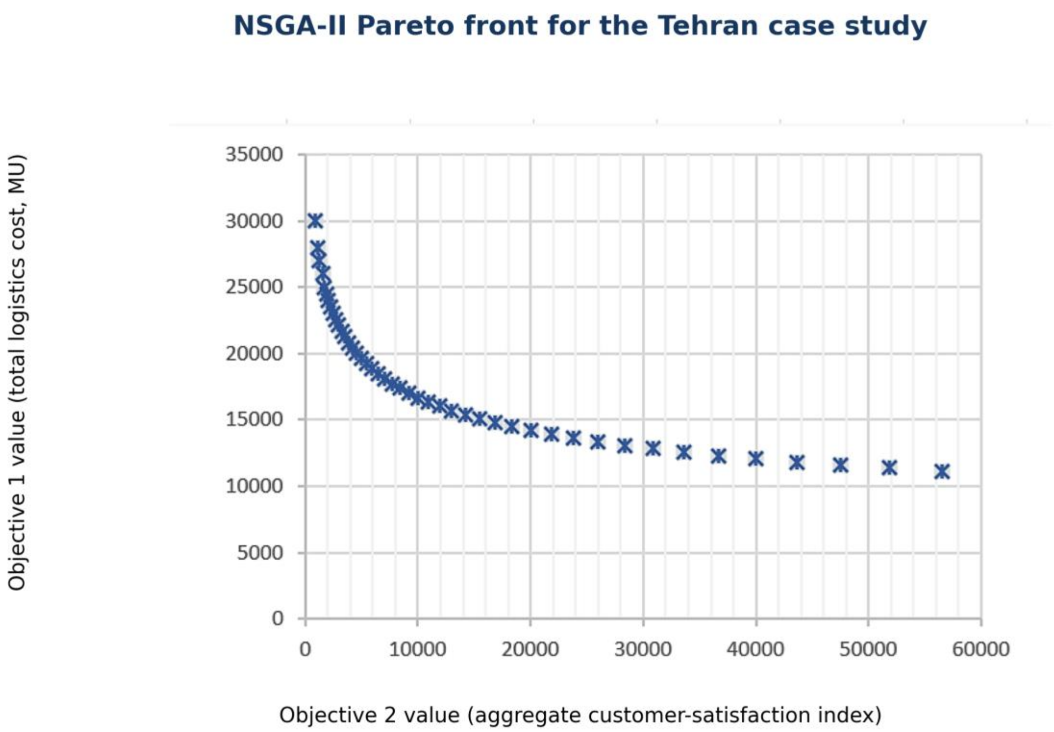

Fig. 12. NSGA-II Pareto front for the Tehran case study.

Table 13. Objective decomposition for the mixed strategy and all-direct baseline.

Dimension	Component	Mixed direct–locker	All-direct	Change under all-direct	Preferred direction
Cost	Time-window penalty	17,021	18,723	+10.0%	Lower
Cost	Distance cost	23,929	27,040	+13.0%	Lower
Cost	Fleet cost	29,885	36,997	+23.8%	Lower
Cost	Locker cost	3,724	0	−100.0%	Lower
Cost	Total z_1	74,559	82,760	+11.0%	Lower
Satisfaction	Time-window score	58,762	52,298	−11.0%	Higher
Satisfaction	Walking-distance penalty	5,104	0	−100.0%	Lower penalty
Satisfaction	Delivery-charge penalty	25,735	28,051	+9.0%	Lower penalty
Satisfaction	Total z_2	27,923	24,247	−13.17%	Higher

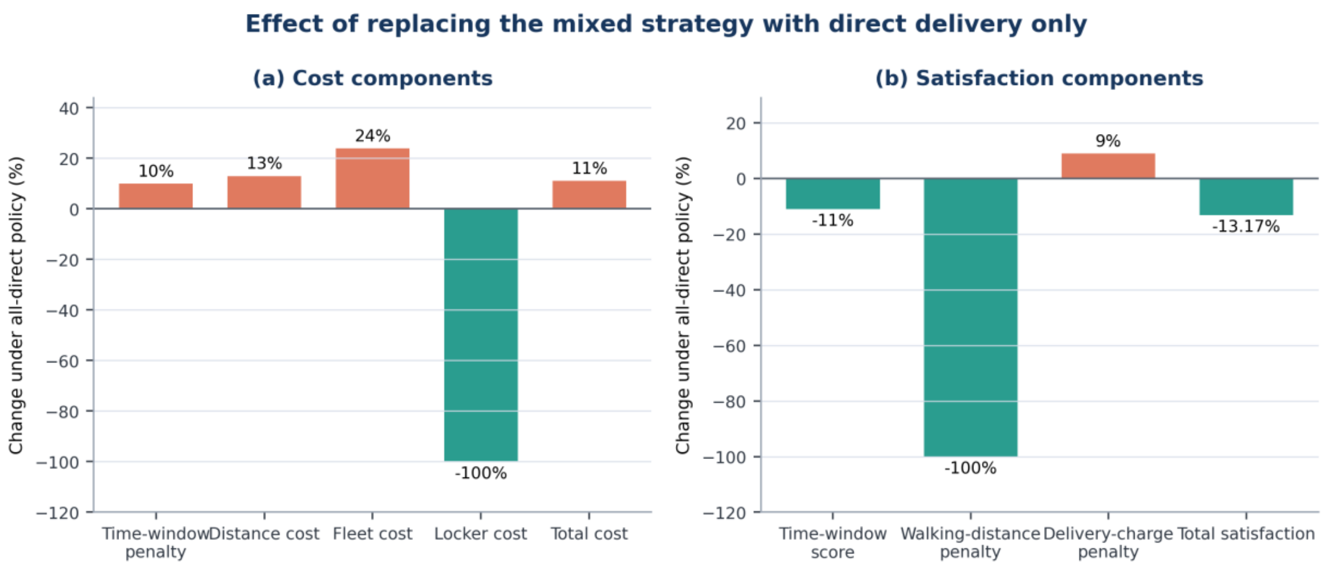

Fig. 13. Percentage changes when the mixed strategy is replaced by direct delivery only.

when the multiplier rises from 0.8 to 1.2, the mixed-strategy cost advantage grows from 7,578.8 to 8,823.2 MU because the all-direct baseline travels more. These calculations are deliberately labeled post-optimal rather than re-optimized sensitivity results; they isolate economic exposure while preserving the integrity of the available numerical record.

5- 7- 2- Locker Coverage Radius

The maximum coverage radius controls both customer accessibility and consolidation. Table 15 and Fig. 15 show that the number of activated lockers declines from 153 at 1 km to 31 at 6 km. A larger radius allows each locker to cover more customers, but the walking-distance penalty makes distant assignments less attractive. The sharp reduction between 2 and 3 km, together with the service-quality trade-off, supports 3 km as an operational upper bound in the case network.

5- 8- Managerial Implications

- Use a mixed channel portfolio rather than treating lockers as a universal substitute for direct delivery. Cold-chain items remain direct, while ordinary products provide the consolidation volume that makes lockers economically attractive.

Table 14. Post-optimal cost checks derived from the case-study component values.

Stress variable	Multiplier	Mixed cost (MU)	All-direct cost (MU)	Mixed-strategy advantage (MU)
Locker cost	0.5	72,697.0	82,760.0	10,063.0
Locker cost	1.0	74,559.0	82,760.0	8,201.0
Locker cost	1.5	76,421.0	82,760.0	6,339.0
Locker cost	2.0	78,283.0	82,760.0	4,477.0
Locker cost	2.5	80,145.0	82,760.0	2,615.0
Locker cost	3.0	82,007.0	82,760.0	753.0
Locker cost	3.2	82,751.8	82,760.0	8.2
Distance cost	0.8	69,773.2	77,352.0	7,578.8
Distance cost	1.0	74,559.0	82,760.0	8,201.0
Distance cost	1.2	79,344.8	88,168.0	8,823.2

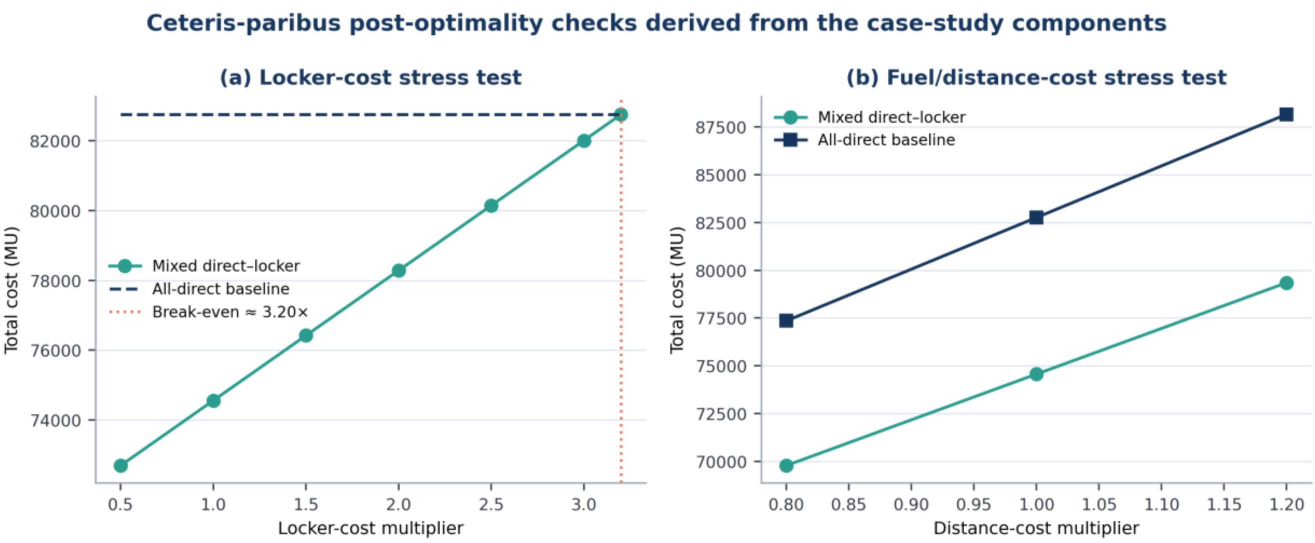

Fig. 14. Locker-cost and distance-cost post-optimality checks.

Table 15. Effect of the maximum coverage radius on locker utilization.

Maximum coverage radius (km)	Activated lockers (count)
1	153
2	149
3	101
4	87
5	45
6	31

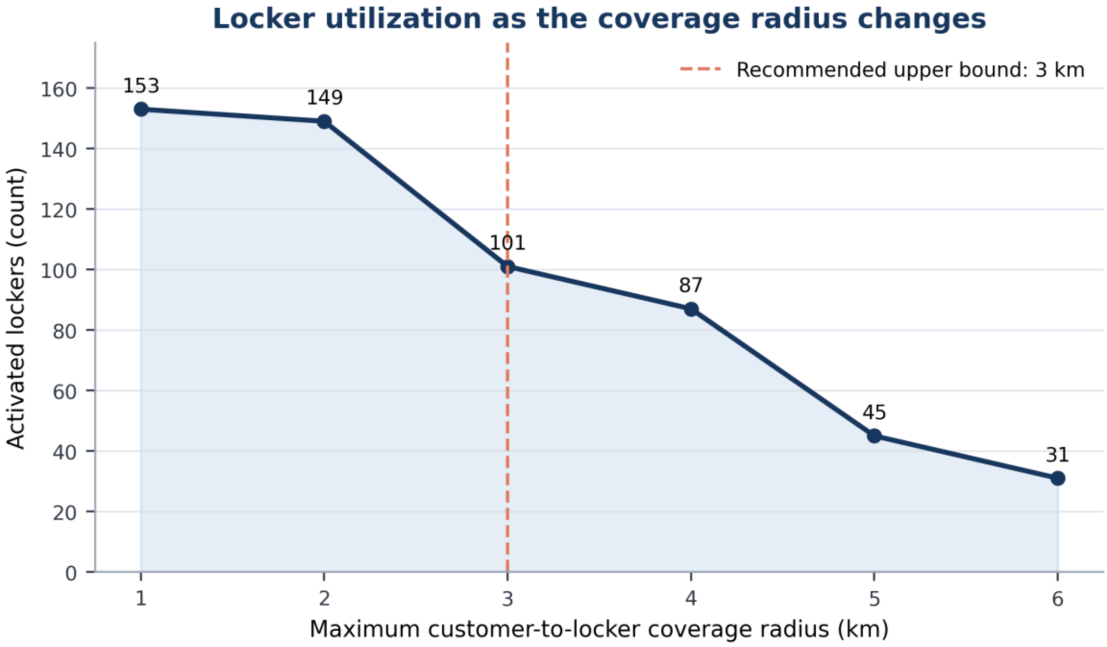

Fig. 15. Effect of coverage radius on the number of activated lockers.

- Reserve fleet capacity centrally but dispatch it adaptively. The two-stage structure avoids paying for scenario-specific overcommitment while retaining enough vehicles to remain feasible under high demand.
- Prioritize lockers within a 3 km customer radius in the Tehran network. Larger nominal service areas reduce the number of active lockers but impose a growing walking-distance penalty and weaken customer acceptance.
- The locker strategy is economically robust. Under the reported component structure, locker cost can rise to approximately 3.20 times its baseline value before the all-direct policy becomes cheaper, and higher distance-related cost strengthens the value of consolidation.
- Present the Pareto front to decision makers instead of selecting a solution through an opaque fixed weight. AEC offers exact anchors for tractable planning studies, while NSGA-II produces a broader set rapidly for operational-scale networks.

6- Conclusions, Limitations, and Future Research

This study develops an integrated decision framework for pharmaceutical last-mile distribution with direct home delivery and smart parcel lockers. Its principal modeling contribution is a bi-objective two-stage stochastic VRPTW in which vehicle reservation and locker activation are fixed before demand is observed, whereas dispatch, routes, visits, service times, delivery channels, and multi-product flows adapt by scenario. The formulation explicitly protects cold-chain products from assignment to non-refrigerated lockers, preserves consolidation through a single locker stop, incorporates simultaneous delivery and returns, and evaluates customer satisfaction through time, walking distance, and delivery charge.

The solution framework combines exact and scalable methods. AEC constructs exact efficient fronts for tractable instances; scenario-aware NSGA-II provides diverse alternatives for larger networks. The paired experiments show that NSGA-II is approximately 4.08 times faster on the five common benchmarks and generates 34.45% more non-dominated solutions on average across 15 instances. AEC, however, achieves a significantly lower MID, while spacing does not differ significantly. The two methods should therefore be viewed as complementary rather than interchangeable.

The Tehran case demonstrates the managerial value of the integrated strategy. Relative to all-direct delivery, the mixed policy reduces cost from 82,760 to 74,559 MU and increases the satisfaction index from 24,247 to 27,923. These changes correspond to an 11% cost increase and a 13.17% satisfaction decrease when lockers are removed. The 3 km coverage recommendation balances consolidation and customer access, and the post-optimal analysis shows that the cost advantage persists until locker cost reaches approximately 3.20 times its baseline value. The research therefore contributes an operational model, an exact–heuristic validation framework, and quantitative guidance for pharmaceutical distributors.

6- 1- Limitations

The model uses three discrete demand scenarios, static orders, non-refrigerated lockers, and one metropolitan case. It therefore does not capture real-time demand and traffic, temperature-controlled locker investment, rare-event probability ambiguity, or geographic transferability; the reported cost stresses are post-optimal rather than fully re-optimized experiments.

6- 2- Future Research Opportunities

Future work can examine refrigerated lockers, data-driven robust or rolling-horizon demand models, and joint siting–routing–pricing decisions. Broader validation may compare additional multi-objective algorithms and incorporate emissions, accessibility, equity, privacy, and chain-of-custody requirements.

References

[1] Aghaei, J., Amjady, N., & Shayanfar, H. A. (2011). Multi-objective electricity market clearing considering dynamic security by lexicographic optimization and augmented epsilon constraint method. Applied Soft Computing, 11(4), 3846–3858. https://doi.org/10.1016/j.asoc.2011.02.022.

[2] Arabatzis, G., Petridis, K., Galatsidas, S., & Ioannou, K. (2013). A demand scenario-based fuelwood supply chain: A conceptual model. Renewable and Sustainable Energy Reviews, 25, 687–697.

[3] Bailey, G., Cherrett, T., Waterson, B., & Long, R. (2013). Can locker box logistics enable more human-centric medical supply chains? International Journal of Logistics Research and Applications, 16(6), 447–460. https://doi.org/10.1080/13675567.2013.856874.

[4] Basso, F., Núñez, M., Paredes-Belmar, G., Pezoa, R., & Varas, M. (2024). Estimation of stops of last-mile delivery vehicles: An application in the food industry in Santiago de Chile. Journal of Transport Geography, 116, 103854. https://doi.org/10.1016/j.jtrangeo.2024.103854.

[5] Deb, K., Pratap, A., Agarwal, S., & Meyarivan, T. (2002). A fast and elitist multiobjective genetic algorithm: NSGA-II. IEEE Transactions on Evolutionary Computation, 6(2), 182–197. https://doi.org/10.1109/4235.996017.

[6] Dell'Amico, M., Montemanni, R., & Novellani, S. (2023). Pickup and delivery with lockers. Transportation Research Part C: Emerging Technologies, 148, 104022. https://doi.org/10.1016/j.trc.2023.104022.

[7] Enthoven, D. L. J. U., Jargalsaikhan, B., Roodbergen, K. J., uit het Broek, M. A. J., & Schrotenboer, A. H. (2020). The two-echelon vehicle routing problem with covering options: City logistics with cargo bikes and parcel lockers. Computers & Operations Research, 118, 104919. https://doi.org/10.1016/j.cor.2020.104919.

[8] Gobir, I. B., Niyang, P. M., Nnadozie, H. O., Agboola, S., Adamu, H., Sanni, F. O., et al. (2024). Acceptability of smart locker technology for dispensing chronic disease medication among patients and healthcare providers in Nigeria. PLOS ONE, 19(3), e0294936. https://doi.org/10.1371/journal.pone.0294936.

[9] Hosseini Shekarabi, S. A., Kiani Mavi, R., Romero Macau, F., Papi, A., & Teymouri, A. (2026). Machine learning-enriched distributionally robust optimization and hybrid decomposition for joint optimization of transportation hub network design and pricing. Computers & Operations Research, 186, 107291. https://doi.org/10.1016/j.cor.2025.107291.

[10] Hovi, I. B., & Bø, E. (2024). Unlocking the potential: How can parcel lockers drive efficiency and environmental friendliness in e-commerce? Sustainable Futures, 7, 100189. https://doi.org/10.1016/j.sftr.2024.100189.

[11] Janinhoff, L., Klein, R., Sailer, D., & Schoppa, J. M. (2024). Out-of-home delivery in last-mile logistics: A review. Computers & Operations Research, 168, 106686. https://doi.org/10.1016/j.cor.2024.106686.

[12] Jiang, L., Chang, H., Zhao, S., Dong, J., & Lu, W. (2019). A travelling salesman problem with carbon emission reduction in the last mile delivery. IEEE Access, 7, 61620–61627. https://doi.org/10.1109/ACCESS.2019.2915634.

[13] Kadadha, M., Mizouni, R., Singh, S., Otrok, H., & Mourad, A. (2024). Crowdsourced vehicles and UAVs for last-mile delivery application using blockchain-hosted matching mechanism. Vehicular Communications, 47, 100761. https://doi.org/10.1016/j.vehcom.2024.100761.

[14] Kim, J., Kweon, S. J., Hwang, S. W., & Lee, S. (2024). Crowdsourcing integration on the last mile delivery platform considering floating population data. Expert Systems with Applications, 248, 123312. https://doi.org/10.1016/j.eswa.2024.123312.

[15] Li, L., Huang, M., Yue, X., & Wang, X. (2024). The strategic analysis of collection delivery points network sharing in last-mile logistics market. Transportation Research Part E: Logistics and Transportation Review, 183, 103423. https://doi.org/10.1016/j.tre.2024.103423.

[16] Lim, J. F. C., Boon, K. G., Ling, C. W. V., Woh, P. T., & Goh, Q. B. (2022). Remodeling the medication collection process with Prescription in Locker Box (PILBOX): Prospective cross-sectional study. Journal of Medical Internet Research, 24(6), e23266. https://doi.org/10.2196/23266.

[17] Liu, Y., Ye, Q., Escribano-Macias, J., Feng, Y., Candela, E., & Angeloudis, P. (2023). Route planning for last-mile deliveries using mobile parcel lockers: A hybrid Q-learning network approach. Transportation Research Part E: Logistics and Transportation Review, 177, 103234. https://doi.org/10.1016/j.tre.2023.103234.

[18] Luo, R., Ji, S., & Ji, Y. (2022). An active-learning Pareto evolutionary algorithm for parcel locker network design considering accessibility of customers. Computers & Operations Research, 141, 105677. https://doi.org/10.1016/j.cor.2021.105677.

[19] Mavrotas, G. (2009). Effective implementation of the ε-constraint method in multi-objective mathematical programming problems. Applied Mathematics and Computation, 213(2), 455–465. https://doi.org/10.1016/j.amc.2009.03.037.

[20] Moradi, N., Sadati, İ., & Çatay, B. (2023). Last-mile delivery routing problem using autonomous electric vehicles. Computers & Industrial Engineering, 184, 109552. https://doi.org/10.1016/j.cie.2023.109552.

[21] Muriel, J. E., Zhang, L., Fransoo, J. C., & Perez-Franco, R. (2022). Assessing the impacts of last-mile delivery strategies on delivery vehicles and traffic network performance. Transportation Research Part C: Emerging Technologies, 144, 103915. https://doi.org/10.1016/j.trc.2022.103915.

[22] Ouyang, Z., Leung, E. K. H., Cai, Y., & Huang, G. Q. (2023). Dynamic community partitioning for e-commerce last mile delivery with time window constraints. Computers & Operations Research, 160, 106394. https://doi.org/10.1016/j.cor.2023.106394.

[23] Pina-Pardo, J. C., Moreno, M., Barros, M., Faria, A., Winkenbach, M., & Janjevic, M. (2022). Design of a two-echelon last-mile delivery model. EURO Journal on Transportation and Logistics, 11, 100079. https://doi.org/10.1016/j.ejtl.2022.100079.

[24] Pinchasik, D. R., Hovi, I. B., & Dong, B. (2023). Replacing home deliveries with deliveries to parcel lockers: Cost, traffic, emissions, and societal cost effects of locker network expansions in greater Oslo. International Journal of Logistics Research and Applications. https://doi.org/10.1080/13675567.2023.2286006.

[25] Pronello, C., Camusso, C., & Rappazzo, V. (2017). Last mile freight distribution and transport operators' needs: Which targets and challenges? Transportation Research Procedia, 25, 888–899. https://doi.org/10.1016/j.trpro.2017.05.464.

[26] Qian, H., Guo, H., Sun, B., & Wang, Y. (2022). Integrated inventory and transportation management with stochastic demands: A scenario-based economic model predictive control approach. Expert Systems with Applications, 202, 117156. https://doi.org/10.1016/j.eswa.2022.117156.

[27] Rabiei, P., Arias-Aranda, D., & Stantchev, V. (2023). Introducing a novel multi-objective optimization model for volunteer assignment in the post-disaster phase: Combining fuzzy inference systems with NSGA-II and NRGA. Expert Systems with Applications, 226, 120142. https://doi.org/10.1016/j.eswa.2023.120142.

[28] Razavi Al-e-hashem, S. A., Papi, A., Pishvaee, M. S., & Rasouli, M. (2022). Robust maintenance planning and scheduling for multi-factory production networks considering disruption cost: A bi-objective optimization model and a metaheuristic solution method. Operational Research, 22, 4999–5034. https://doi.org/10.1007/s12351-022-00733-x.

[29] Risberg, A. (2022). A systematic literature review on e-commerce logistics: Towards an e-commerce and omni-channel decision framework. International Review of Retail, Distribution and Consumer Research. https://doi.org/10.1080/09593969.2022.2089903.

[30] Seghezzi, A., Siragusa, C., & Mangiaracina, R. (2022). Parcel lockers vs. home delivery: A model to compare last-mile delivery cost in urban and rural areas. International Journal of Physical Distribution & Logistics Management, 52(3), 213–237. https://doi.org/10.1108/IJPDLM-03-2020-0072.

[31] Shi, Y., Lin, Y., Li, B., & Li, R. Y. M. (2022). A bi-objective optimization model for the medical supplies' simultaneous pickup and delivery with drones. Computers & Industrial Engineering, 171, 108389. https://doi.org/10.1016/j.cie.2022.108389.

[32] Vukićević, M., Ratli, M., Rivenq, A., & Zrikem, M. (2023). Covering delivery problem with electric vehicle and parcel lockers: Variable neighborhood search approach. Computers & Operations Research, 157, 106263. https://doi.org/10.1016/j.cor.2023.106263.

[33] Wang, Y., Bi, M., Lai, J., Wang, C., Chen, Y., & Holguín-Veras, J. (2024). Recourse strategy for the routing problem of mobile parcel lockers with time windows under uncertain demands. European Journal of Operational Research, 316(3), 942–957. https://doi.org/10.1016/j.ejor.2024.02.034.

[34] Wei, L., Chen, Y., Guo, D., Ji, J., Chen, Z., & Zhuo, C. (2024). A last-mile delivery system for underground logistics with 'self-pickup +' and 'home-entry +' modes. Tunnelling and Underground Space Technology, 147, 105678. https://doi.org/10.1016/j.tust.2024.105678.

[35] Wets, R. J.-B. (1994). Challenges in stochastic programming. International Institute for Applied Systems Analysis, Laxenburg.

[36] Yeo, Y.-L., Chang, C.-T., Chew, C.-C., & Rama, S. (2021). Contactless medicine lockers in outpatient pharmacy: A safe dispensing system during the COVID-19 pandemic. Research in Social and Administrative Pharmacy, 17(5), 1021–1023. https://doi.org/10.1016/j.sapharm.2020.11.011.

[37] Yu, V. F., Susanto, H., Yeh, Y.-H., Lin, S.-W., & Huang, Y.-T. (2022). The vehicle routing problem with simultaneous pickup and delivery and parcel lockers. Mathematics, 10(6), 920. https://doi.org/10.3390/math10060920.

[38] Yu, Y., Lian, F., & Yang, Z. (2021). Pricing of parcel locker service in urban logistics by a TSP model of last-mile delivery. Transport Policy, 114, 206–214. https://doi.org/10.1016/j.tranpol.2021.10.002.

[39] Zhou, L., Li, C., Hu, C., & Du, J. (2023). Parcel locker location problem with selectable volume sizes and heterogeneous customers in last-mile delivery. Transportation Letters. https://doi.org/10.1080/19427867.2023.2277013.

[40] Zhu, W., Hu, X., Pei, J., & Pardalos, P. M. (2024). Minimizing the total travel distance for the locker-based drone delivery: A branch-and-cut-based method. Transportation Research Part B: Methodological, 184, 102950. https://doi.org/10.1016/j.trb.2024.102950.

[41] Zitzler, E., Deb, K., & Thiele, L. (2000). Comparison of multiobjective evolutionary algorithms: Empirical results. Evolutionary Computation, 8(2), 173–195. https://doi.org/10.1162/106365600568202.

HOW TO CITE THIS ARTICLE

R. Shafiee Aghdam, M. Akbarpour Shirazi, B. Karimi, Innovative Vehicle Routing Strategies for Pharmaceutical Distribution Using Parcel Lockers: A Bi-objective Two-Stage Stochastic Approach, AUT J. Model. Simul., 58(1) (2026) 67-94.

DOI: 10.22060/miscj.2026.24244.5413